Variable sample density at high b-values for Radial Diffusion Spectrum Imaging improves angular resolution

Steven Baete[1,2] and Fernando Emilio Boada[1,2]

[1]*Center for Advanced Imaging Innovation and Research (CAI2R), NYU School of Medicine, New York, NY, United States,* [2]*Center for Biomedical Imaging, Dept. of Radiology, NYU School of Medicine, New York, NY, United States*

Target audience Scientists and clinicians interested in Diffusion Spectrum MRI, its methodological development and the sampling of the ODF.

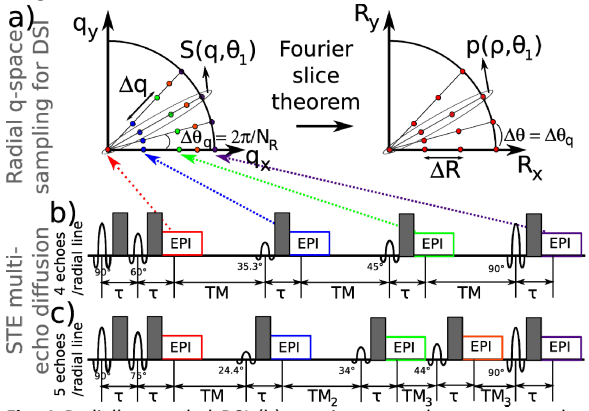

Fig. 1 Radially sampled DSI (b) acquires several q-space samples (e.g. 4 or 5) along several radial lines. This is most efficiently done with a multi-echo stimulated echo diffusion sequence which naturally acquires several (e.g. 4 or 5) echoes along the same radial line in q-space in one readout. Once acquired, each radial line in q-space can be transformed to the value of the ODF at the same radial line using the Fourier slice theorem (b).

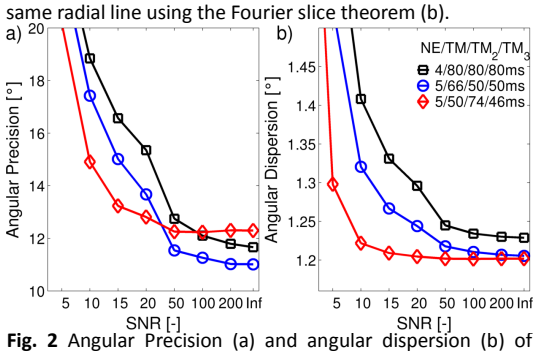

Fig. 2 Angular Precision (a) and angular dispersion (b) of RDSI with 4 and 5 echoes as a function of SNR (b_{max}=4000), calculated from simulated ODF's of one and two crossing fibers (random angles).

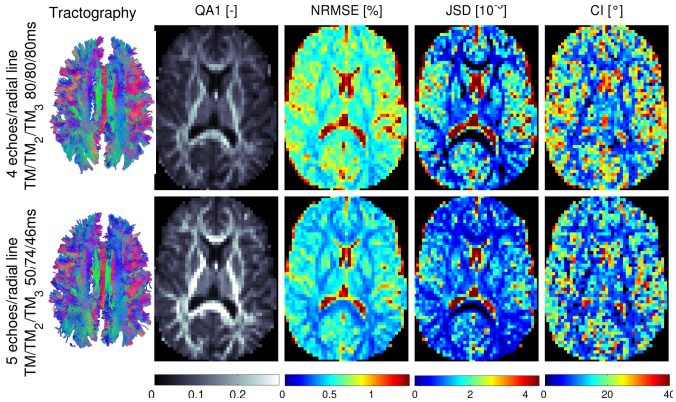

Fig. 3 Radial DSI reconstructions of a human brain volunteer acquired using a multi-echo stimulated echo sequence with 4 and 5 echoes. Shown are tractography results of the central 10 slices, quantitative anisotropy (QA)[14] of the prominent fiber orientation, NRMSE and JSD relative to the average ODF and the 95% Confidence Interval (CI).

Purpose To demonstrate the improved ODF sampling and angular resolution of Radial Diffusion Spectrum Imaging (RDSI) when using optimized variable q-space density acquisitions.

DSI [1] has been shown to have superior performance for non-invasively imaging the white matter tract architecture of the human brain, especially when complex intravoxel fiber crossings are present [2,3]. DSI's improved performance results from the model-independent determination of the Orientation Distribution Function (ODF) through direct measurement of its Fourier transform in q-space [1]. Improved depiction of intravoxel crossings is, therefore, directly related to the angular resolution afforded by the sampling raster in q-space [4].

For a fixed number of samples, radial q-space sampling for DSI [5,6] (RDSI, Fig 1a) has been shown to provide improved angular resolution over its conventional Cartesian counterpart. In addition, the q-space sampling scheme (Fig 1a) in RDSI lends itself naturally to a multi-echo stimulated echo acquisition approach where multiple samples are acquired along a radial line in one single TR (Fig 1b), which leads to improved acquisition speed [7]. A further improvement in the angular resolution for RDSI can be reached by adapting the sample density in q-space (Fig 1b), so that the noise variance can be minimized [8]. This approach significantly improves the SNR of the reconstructed ODF when higher b-values are used without increasing the scan time. In this work, we demonstrate the benefit of this approach with reproducibility metrics of bootstrapped *in vivo* RDSI datasets acquired in a clinical 3T scanner.

Methods RDSI datasets were acquired with a custom-made, multi-echo, stimulated echo EPI diffusion sequence [7,9](Fig 1b and 1c) using a recently proposed radial q-space sampling scheme (Fig 1a) [5,6] (Fig 1a; 4 or 5 q-space samples along each of 59 radial lines evenly distributed on a half sphere, 236/295 samples in total). Optimal sequence timing configurations (i.e. choice of TM, TM2 and TM3 (Fig 1b)) were chosen based on simulations of angular precision and dispersion [10](Fig 2), the latter being a measure of angular accuracy. The simulations studied two crossing fibers with random directions and a water pool (10%) under added Rician noise.

Datasets were acquired of healthy volunteers on a 3T clinical scanner (Skyra, Siemens, Erlangen; 20ch head coil; b_{max}=4000, TR=4000, 3×3×3mm, 10 slices, TE=48,152,256,360/48,122,220,290,360ms (4/5 echoes). Each timing configuration (4/5 echoes) was acquired 4 times during the same session (4:24min/scan), alternating between timing configurations. These 4 original datasets were then used to generate 500 bootstrap datasets using repetition bootknife sampling [11]. The resulting bootstrapped ODFs are used to calculate the normalized RMSE (NRMSE) and Jensen-Shannon Divergence (JSD) [11] relative to the mean ODF and 95% Confidence Interval (CI)[12] of the identified main fiber direction. RDSI reconstructions, incorporating variable q-space sample density correction, were performed offline using custom-made software (Matlab, Mathworks) and displayed using Matlab and DSI Studio [13].

Results and Discussion The simulation results in Fig 2 illustrate the improved angular precision and dispersion of the variable q-space density approach when used in conjunction with a multi-echo STE sequence. As expected, the improvement increases as the SNR levels decrease [8]. The findings from the simulations are also reproduced when observing the *in vivo* bootstrap data (Fig 3) as demonstrated by the decreased NRMSE, JSD and CI. The advantage of variable q-space sampling density is already apparent at the higher SNR level of this dataset (SNR of the first b_0 echo 190), suggesting an even larger improvement for lower SNR (Fig 2). The *in vivo* tractography results and Quantitative Anisotropy maps are similar, except that the reconstruction of the variable density dataset yields higher QA-values, which leads to improved tractography results.

Conclusion RDSI acquired with a multi-echo stimulated echo diffusion sequence benefits significantly from the use of variable density in q-space. Our results demonstrate improved angular resolution and ODF reproducibility without an increase in acquisition time. These findings, combined with earlier published results [5,6], showing the improved angular resolution of RDSI over conventional Cartesian sampled DSI, suggest that variable sampling in RDSI has definite advantages over Cartesian DSI.

Funding NIH 1NS082436-01A1, NIH 2R01CA111996-06A1 and NIH R01 MH088370. References [1] Callaghan P., Principles of NMR Microscopy, Oxf. Univ. Press, 1993. [2] Wedeen VJ, et al., Science, 335:1628,2012. [3] Fernandez-Miranda JC, et al., Neurosurg., 71:430, 2012. [4] Wedeen VJ, et al., MRM 54:1377, 2005. [5] Boada FE, et al., Proc ISMRM, p3177, 2013. [6] Baete S, et al., Proc ISMRM, p663, 2014. [7] Baete S, et al., Proc ISMRM, p88, 2014. [8] Boada F, et al., MRM, 38:1022-1028, 1997. [9] Franconi F, et al., JMRI 7:399-404, 1997. [10] Kuo LW, et al., NeuroImage 29:517-22, 2008. [11] Cohen-Adad, et al., JMRI 33:1194-1208, 2011. [12] Jones DK, et al. MRM 51:807-15, 2004. [13] Yeh FC, et al., IEEE TMI 29:1626, 2010. [14] Yeh FC, et al., IEEE TMI 54:1377-1386, 2005.